AUTOMATED MINERAL IDENTIFICATION OF SANDSTONE SAMPLES USING SEM/IMAGE ANALYSIS TECHNIQUES

Theo W. Fens, Jos H.M. Bonnie & William D. Clelland Shell Research, Rijswijk (Koninklijke/Shell Exploratie & Produktie Laboratorium)

Abstract A combination of scanning electron microscopy, X-ray analysis and image analysis (SEM/EDX/IA) has been used to perform automatic petrographic analysis of sandstone samples. The methods developed involve the use of backscattered electron (BSE) imaging and X-ray analysis together with image analysis procedures to determine and to quantify the mineralogical composition and grain texture information. The samples to be investigated can be core plugs, sidewall samples or cuttings. Prior to analysis the samples are impregnated with epoxy resin and subjected to high-quality automatic polishing.

The analysis procedure starts with the collection of a BSE image from the SEM, this image is stored in the memory of the image analysis system. Thereafter the locations of the grains and mineral structures in the image are determined and converted to coordinates on the sample surface. The individual grains and mineral structures are then scanned with the electron beam of the SEM. During the scanning of the individual objects, X-rays are generated, and these are detected and analysed in terms of their elemental information. This information is subsequently used to identify the mineralogical composition of these objects. An image is generated in which the composition of the individual grains and

[©] Shell Research B.V. The Netherlands. With permission

mineral structures is indicated by a colour code. Finally, image analysis is used to quantify the amount of the various minerals present and the geometry of the grains and mineral structures. The procedures are fully automated and, once set up, can be run without operator involvement (overnight, for example). A wealth of quantitative data can be obtained using this single approach, which provides information useful in many fields of petroleum engineering (such as diagenetic studies and the prediction of (petro)physical properties). An example is given of an application in the area of well stimulation, in which the influence of acid formulation on reservoir rock is studied.

INTRODUCTION

Mineral identification is a tool that is used in various areas of reservoir assessment: in diagenetic studies, in determining petrophysical properties and in studying the effect of stimulation exercises, acidisation, for instance.

Conventionally, X-ray diffraction, infra-red analysis or thin-section analysis is used to assess the mineralogical content of reservoir rock. The level of information of these mineralogical reservoir descriptions is often constrained by our limited capacity to characterise features in a quantitative manner. Thin-section point-counting is the spatial analysis technique which relates to the procedures described below. Point-counting can provide only semi-quantitative data, is rather labour-intensive and, by definition, subjective.

With the availability of an integrated analysis system consisting of SEM/EDX/IA (scanning electron microscopy, X-ray analysis and image analysis) the way was opened to design and develop a fully automated procedure for assessing the mineralogical composition and pore structure of reservoir rock. The objective was to provide information on the mineralogical composition and pore structure on the same

scale as thin-section analysis but in a more reproducible, consistent and quantitative manner. This means that the procedure should be automated as much as possible and preferably based on established technology and physics. This procedure will be explained in the following.

The instrumentation and its principles will de described briefly, together with some of the underlying physics. The procedures for image collection, object definition, object scanning, X-ray data collection and classification will be discussed. Example studies on reservoir rock from various lithologies will be presented. Finally, conclusions and recommendations concerning future research in this area will be indicated.

INSTRUMENTATION AND PRINCIPLES

Equipment and Sample Preparation

The equipment employed in this evaluation procedure consists of three main parts which are all interfaced: a Philips 515 scanning electron microscope (SEM), a Kevex Analyst 8000 energy-dispersive X-ray analyser (EDX) and a Kontron SEM-IPS image-processing system (IPS). Under fully automated operation the IPS host computer controls all pertinent functions of both the SEM and the EDX.

Scanning electron microscopy is an established technique in geological evaluation, by which means the surface of small pieces of rock can be visualized and investigated. To this end the fractured surface of a piece of reservoir rock is scanned with an electron beam under high-vacuum conditions. The electrons emerging from this surface during scanning are detected and used to build up an image. Because the amount of emerging electrons reflects the structure of the surface, the morphology of this surface can be visualized. An image of this type can be seen in Figure 1, in which the blocky structures are dolomite rhombs overgrown

on quartz grains. The platelets which can be observed are kaolinite booklets. Although these types of images reveal surface structure in detail, parameters describing these images cannot easily be quantified because of the 3-D nature of these fractured surfaces.

A solution to providing quantitative data from reservoir rock was found in the use of polished blocks. In the preparation, slices from drilled core plugs are impregnated with epoxy resin under vacuum conditions, to ensure that even very small pores become filled. SEM investigation showed that pore spaces between kaolinite booklets down to 50 nm were filled. The epoxy system used was selected on the basis of properties such as wettability, low shrinkage in curing, low viscosity during impregnation and comparable with that of minerals. The last characteristic is necessary because the samples are subjected to high-quality after impregnation. The five-stage polishing polishing procedure is fully automatic and is performed on one single machine. The total polishing procedure takes about 45 minutes for a set of three samples. After being polished, the samples are coated with a thin carbon layer (approx. 100 nm), to provide a conductive surface, and brought into the SEM.

The main techniques employed in this evaluation procedure are BSE (backscattered electron) imaging and X-ray analysis. A brief outline of the principles of these techniques is given below. In the following sections their use, in conjunction with image analysis procedures (Serra, 1982), in determining rock parameters automatically from resinimpregnated and polished samples will be discussed.

Backscattered Electron Imaging

The electron beam that scans the samples surface not only generates secondary electrons that are used in conventional broken sample analysis, but also causes a flux of backscattered electrons that can be detected separately. The signal provided by the BSE detector reflects the average

atomic number at the analysis spot on the sample (Hall and Lloyd, 1981). Figure 2a shows a BSE image of a sandstone sample in which the grey level is related to the average atomic number of the mineral, such that the denser the mineral is, the brighter it appears. The pores are dark because they are filled with a low-density epoxy resin.

From such an image the image analyser can recognise the pore space or particular groups of minerals by detecting only those areas whose grey level falls within a specified range. This procedure is known as grey-level segmentation or thresholding (Figure 2b). Such a technique has previously been used to obtain mineralogical information (Dilks and Graham, 1985). However, because different minerals can have similar average atomic numbers (for instance, quartz, dolomite and sodium feldspar) the segmentation enables partial discrimination only. To distinguish such minerals X-ray analysis must be used.

X-ray Analysis

The EDX system measures the X-ray energy spectrum, i.e., the intensity and the energy of the X-rays generated by the interaction of the electron beam and the sample.

The spectrum consists of two parts: (1) a continuous (background) signal which is not used in the mineral identification procedure and (2) characteristic lines representative of certain elements. Detection and classification of the characteristic X-ray lines enables the elements present at the analysis spot to be identified. In addition, the number of X-rays emitted by each element is related to the concentration of that element.

The Data Collection and Analysis Procedure

The automated procedure is shown schematically in Figure 3. After the sample preparation and BSE image collection with the SEM and the IPS, it involves the recognition of individual objects (i.e., grains, diagenetic minerals,



FIGURE 1 SEM secondary electron image showing surface structure of a shaly sandstone at 500 X magnification. The white scale bar is 100 $\mu m.$ Note the kaolinite booklets upper left and the dolomite rhombs in the centre.

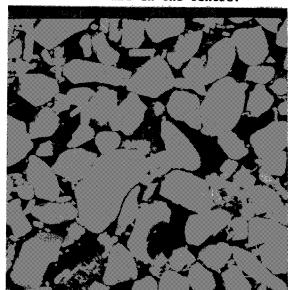


FIGURE 2a BSE image of a sandstone at a magnification of 100%. The yellow size reference lower right is approx. 100 μ m. Brightness is proportional to the atomic number. The field size is 1.8 x 1.8 mm in 512 x 512 points.

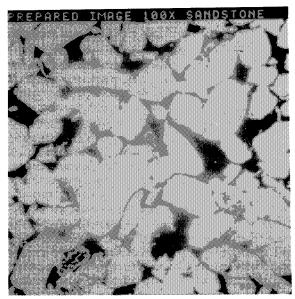


FIGURE 2b Discriminated image derived from Figure 2a in which the grains and mineral structures are separated from the pores on the basis of grey level

(See Colour Plate IV at the back of this publication.)

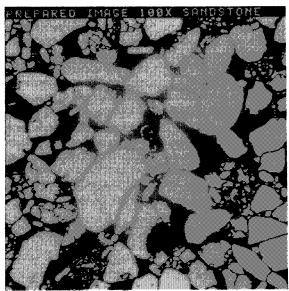


FIGURE 2c Segmented image derived from Figure 2b. Image processing is used to define the individual grains and mineral structures.

(See Colour Plate V at the back of this publication.)

clays) in the sample. X-ray analysis is then carried out on each object to obtain elemental data which can be classified in terms of mineralogy. The individual objects can also be analysed with respect to their size, shape, etc. The complete procedure consists of a number of steps which are described below.

Image acquisition

A BSE image from the SEM is digitized and stored in the memory of the IPS. The stored image has a standard format of 512×512 points (or pixels = picture elements) in which each point can have a grey value from 0 to 255. The value 0 corresponds to black (pores) and ranges through grey (quartz) to white (heavy minerals), which is 255. Typically, these images are collected from an area (field of view) of 1.8×1.8 mm on the sample surface.

Grain detection

In BSE images of sandstone samples the grain edges and grain-to-grain contacts often have a darker appearance than the grain interiors, as can be seen in Figure 2a. However, the grain-to-grain contacts are sometimes not visible along their complete length, see Figure 2b, particularly in well-consolidated samples. To define the individual grains better, a number of morphological operations (Serra, 1982) have been used. These have been described previously (Clelland et al., 1990) and result in processed images such as shown in Figure 2c. From such an image it is possible to obtain various textural parameters (e.g., grain size distribution, shape).

Object scanning

The objects in the image can now be recognised and the IPS takes control of the microscope and scans the beam over the area of each object in turn. During this procedure, X-rays are generated. An X-ray spectrum of each object is obtained in which 9 energy windows are predefined. The X-ray counts in the windows are normalised and sent to the IPS as a vector of nine elements (Na, Mg, Al, Si, P/Zr, K, Ca, Ti/Ba, Fe). (Note that the energies of the characteristic lines of P and Zr and of Ti and Ba overlap and so these elements cannot be uniquely identified.) In the IPS the contribution of the background is removed prior to the mineral classification.

Mineral/textural identification procedure

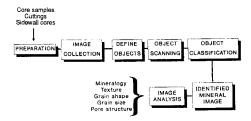


FIGURE 3 Outline of the mineral identification procedure

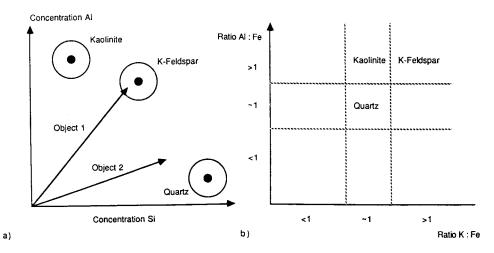


FIGURE 4a Simplified mineral classification procedure in which rough concentrations based on X-ray analysis are used

FIGURE 4b Simplified mineral classification procedure in which pseudo elemental ratios are used to reduce statistical fluctuations and X-ray collection time

Mineral classification

The classification of each object or grain is done by comparing the X-ray counts obtained from the unknown mineral with those of known reference minerals. A simplified procedure is shown in Figure 4a, in which the concentrations of Si and Al (roughly proportional to the X-ray counts at appropriate energies) are used to classify some silicate minerals. In the actual classification procedure the complete vector of nine elements is used to enable discrimination between a greater number of minerals. This procedure worked successfully for many minerals, problems were encountered in classifying minerals whose composition could vary slightly. For example, dolomite can contain minor amounts of iron. However, if the X-ray counts from such a grain are compared with those of a "pure" the data may differ too much to enable classification. To define a reference composition for every subvariety of a mineral would be an extremely difficult if not impossible task. Another problem with this method is that statistical fluctuations in the data can result in the misclassification of some minerals, and considerable analysis time is required to resolve this problem. Given the above problems, a new method has been developed in which elemental ratios are used instead of absolute elemental concentrations. Elemental ratios (X:Y, say) are converted to pseudo elemental ratios using the following approach:

- (1) If the concentration of element X is found to be somewhat higher than element Y, then a value of 2 is given to the pseudo ratio.
- (2) If the concentration of element X is found to be somewhat lower than element Y, then a value of 0 is given to the pseudo ratio.
- (3) If the two elements, X and Y, are found to exist in similar concentrations in the mineral, or if they are not present, then a value of 1 is given to the pseudo ratio. Errors can be caused by noise fluctuations in the X-ray spectrum. This might be mistaken for elements occurring in very low concentrations. To avoid this a certain threshold above the noise level concentration has to be reached before an element is considered as being present.

A set of reference minerals is listed in Table 1 together with the appropriate values of pseudo elemental ratios for a number of pairs of elements. In the classification procedure the pseudo elemental ratios of an unknown grain are compared

Table 1 - Pseudo elemental ratios used in mineral classification

	Fe·K	K·Ti/Ra	Cars	P/Zr:Al	Ma:Si	K · Al	Fe:Ca	SitAl
Albite	1	1	1	0	0	0	1	2
Anhydrite/	*	-	•	Ū	·	·	-	-
	1	1	1	1	1	1	0	1
Gypsum	_	1	1	1	-	-	_	1
Ankerite	2	1	2	1	2	1	0	1
Apatite	1	1	2	2	1	1	0	1
Baryte	1	0	0	1	1	1	1	1
Biotite	2	2	1	0	0	1	2	2
Calcite	1	1	2	1	1	1	0	1
Dolomite	1	1	2	1	2	1	0	1
Kaolinite	1	1	1	0	0	0	1	1
Orthoclase	0	2	1	0	0	2	1	2
Pyrite	2	1	0	1	1	1	2	1
Quartz	1	1	1	1	0	1	1	2
Rutile	1	0	1	1	1	1	1	1
Zircon	1	1	1	2	0	1	1	2
Anorthite	1	1	2	0	0	0	0	2
Halite	1	1	1	1	1	1	1	1
Hematite	2	1	1	1	1	1	2	1
Illite/								
Muscovite	0	2	1	0	0	0	1	2
Sphene	1	0	2	1	0	1	0	2
IF Ratio	< 0.75 THEN Ratio = 0							
IF 0.75	≤ Rá	atio ≤ :	1.33	THEN F	Ratio =	: 1		

IF 1.33 < Ratio THEN Ratio = 2

with those of the reference minerals. Figure 4b shows a simplified procedure using two elemental ratios (K:Fe and Al:Fe) to classify some silicate minerals. The quartz does not contain any Al, K or Fe and so both ratios are defined as 1. Kaolinite contains Al but not K or Fe and so the Al:Fe ratio is defined as 2 and the K:Fe ratio as 1. Potassium feldspar contains both Al and K but no Fe, so both ratios are defined as 2.

With the new method, statistical fluctuations have less influence on the classification, and the analysis time for each grain can be reduced from 10 seconds to 3 seconds. It is also possible to take into account slight variations in composition without having to define a large number of reference compositions for each mineral. Figure 5a shows the result of classifying the grains detected from the BSE image of Figure 2a. The different colours represent the different mineral classes considered, see Figure 5b. Measuring the area of the pores and various minerals can then easily be

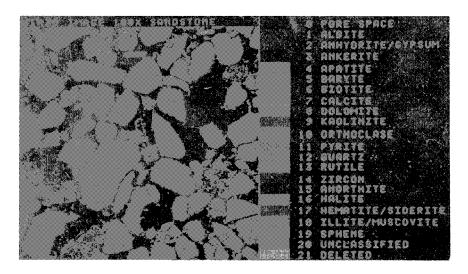


FIGURE 5a Mineralogically classified image derived from Figure 2a, the colours are indicative of the mineral found on the basis of X-ray analysis (See Colour Plate VI at the back of this publication.)

FIGURE 5b Reference for the colours in Figure 5a

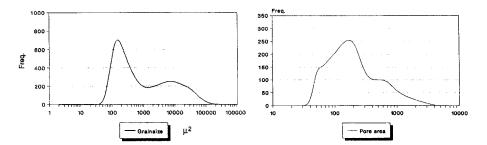


FIGURE 6a 2-D grain size distribution from the sample in Figure 5a, the grain size being defined as the area of each object

FIGURE 6b 2-D pore size distribution from the same sample, pore size being defined as the area of each individual pore

carried out. For homogeneous samples, these measurements are equivalent to the volume fractions of the individual minerals.

This technique does not enable discrimination between certain minerals, e.g., hematite and siderite, with the elements listed in the table. This is because carbon and oxygen have not been taken into account in the analysis. However, by removing the 8 μm thin beryllium window in front of the X-ray detector (a simple procedure), it is possible to analyse these elements, enabling a greater number of minerals to be discriminated.

The mineral file shown in Table 1 is for general use. Other files can be constructed containing sets of minerals suited to specific groups of samples or to enable detailed discrimination within a certain group of minerals (e.g., carbonate minerals).

Pore structure analysis

In the analysis procedure objects such as grains, clay regions and cementation were geometrically defined to enable scanning with the electron beam. Since these objects are now readily available in the image, analysis makes it possible to describe them in geometrical terms, i.e., in size and shape parameters. An example is shown in Figure 6a, in which the 2-D grain size distribution from Figure 5a is presented. The grain-size is defined as the area of each grain. A similar procedure can be used in determining the 2-D pore size distribution from the pore network extracted, as can be seen in Figure 6b.

It should be noted that these geometrical parameters are obtained from sections and cannot always easily be related to reservoir parameters such as permeability which are 3-D in nature (Weibel, 1980). Efforts are under way to investigate the relationship between 2-D geometry and 3-D reservoir parameters. Some type of modelling is required to establish this relationship. Discussion of these efforts is

beyond the scope of this paper and will be published in literature separately.

Automation

The procedures discussed here are all linked and can be applied to the analysis of one field of view. However, to enable the analysis of more fields of view, it is necessary to move the sample. This is done by a motor-driven scanning stage mounted on the SEM, and this can be remotely controlled from the IPS. Before the procedure is started, the coordinates of the fields to be analysed are stored in the memory of the IPS. This means that the analysis of a number of fields of view or samples can be performed in one run without operator interaction (for instance, overnight).

IMPROVEMENTS

In comparison with the previously published method (Fens & Clelland, 1990), the present procedure is an improvement in a number of areas:

The sample preparation procedure:

An impregnation method under vacuum at elevated temperature has been developed. This provides better preservation of delicate clay structures such as kaolinite and illite. The grinding and polishing is done fully automatically and requires less than 30 minutes per sample, which ensures a short turn-around time. In addition, the polishing is of superior quality to that obtained with the previous, partly manual procedure.

New image-processing algorithms:

The geometrical accuracy has been improved by implementing newly developed image-processing algorithms.

For one thing these enable the classification of small rims around grains, i.e., clay coatings, which was hitherto not possible. The spatial resolution for clay rims that can now be analysed is in the order of several micrometres. Thinner clay rims are still not resolved by this technique. Note that clay analysis solely on the basis of chemical (elemental) constituents might lead to erroneous results because of the variable composition of the clays. A possible solution to this is to incorporate clay textural data in the analysis. This is currently under investigation. Another substantial improvement has been achieved in the analysis of cementation. different generations of the cementation can be segregated on the basis of grey level, and these are then analysed individually, resulting in a more accurate classification. This can be clearly observed in the upper left region in Figures 7a and 7b, in which the micaceous structure is separated in a biotite part and a muscovite part.

More accurate X-ray data by means of a better correction procedure:

When an individual object is scanned with the electron beam, an X-ray spectrum is collected which contains elemental information of that particular object. This spectrum has to be corrected for background effects which can influence the quantification dramatically. The static background correction which uses a fixed correction function was replaced by one with a dynamic offset control, for which the offset of the correction function is dependent on the counting statistics in the spectrum. In this way more accurate data are obtained, which leads to a better elemental analysis and mineral classification.

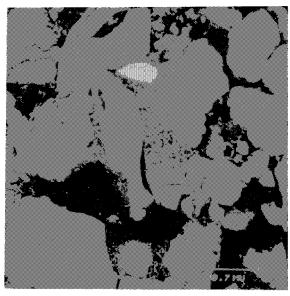


FIGURE 7a BSE image of a sandstone at a magnification of 100%. The size reference is approx. 100 μm_{\star}

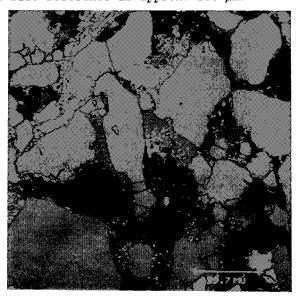


FIGURE 7b Mineral image derived from Figure 7a. Note the micaceous structure in the upper left of the image, biotite in yellow and muscovite in pink.

(See Colour Plate VII at the back of this publication.)

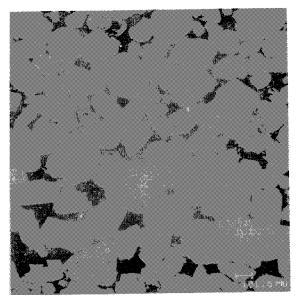


FIGURE 8a BSE image of a high-porosity, slightly arkosic sandstone, magnification $50\ensuremath{\mathrm{X}}$

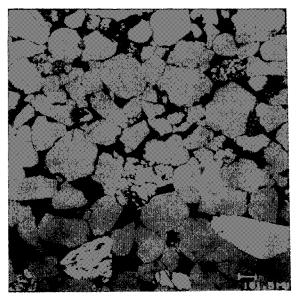


FIGURE 8b Mineral image derived from Figure 8a (See Colour Plate VIII at the back of this publication.)

More accurate mineralogical classification:

The classification algorithm itself has been extended, enabling a more accurate mineralogical identification. The existing algorithm was based on the ratio method, which uses elemental ratios to classify the mineralogical composition of an object. In some cases this leads to unclassified objects. In particular, clays and detrital grains with a spatially variable composition (lithics) cannot be classified properly using the ratio method. In an attempt to resolve this issue, a second algorithm was appended to the existing one. In this algorithm the elemental vector of each individual grain or object is compared with a set of vectors obtained from standard minerals under identical microscope conditions. The combination of the two methods enables a more complete determination of the mineralogical composition of clastic samples at the cost of a longer analysis time. This time is increased from some 30 minutes per field of view to about one hour per field of view, depending on the mineralogical complexity of the sample. On average a field of view contains approximately 500 to 800 objects to be analysed and classified. Although the longer analysis time is a disadvantage, this is fully compensated by the much better results, particularly for samples with a complicated mineralogical composition.

EXAMPLES FROM VARIOUS LITHOLOGIES

To show the robustness of the developed technique, two samples, each with a different mineralogical nature, were subjected to automated mineral analysis. Figure 8a shows the BSE image of a high-porosity, slightly arkosic sandstone. Dolimite cement can be observed between the grains in green in the lower right on the mineral image in Figure 8b. Pore-filling kaolinite can be seen in a large pore

(approximately 100 μm diameter in this image) near the right edge of Figure 8b. Potassium feldspar grains $% \left(1\right) =0$ are presented in blue.

A somewhat more shaly sample, the BSE image of which is presented in Figure 9a, was also analysed. The abundant clay type was found to be illite, shown in pink. In comparison with the previous sample, more dolomitic cement was observed with ankerite rims, which are presented in red around the green dolimite. In the middle left on Figure 9b pyrite cement can be seen in dark blue.

One field application of the mineral identification technique was its use in a well stimulation exercise. Acid formulation for well stimulation by matrix acidising is best chosen on the basis of detailed knowledge about reservoir mineralogical composition. The identification technique was used on core samples before and after laboratory acid reponse tests to assist in the design of the acid programme to be followed in the field (Nitters & Hagelaars, 1990). In this manner it was possible to tune the acid formulation optimally to the reservoir mineralogical composition and to obtain maximum effect of the acid treatment. Details of this study were described by Nitters and Hagelaars, 1990. The problem to be solved was to improve the permeability of a shaly, calcareous sandstone, without the collapse of the matrix structure. Figure 10a and 10b show the BSE image and the mineral image of the untreated rock. Note the high amount of calcite cement shown in beige. After treatment with RMA (regular mud acid), the majority of calcite cement was dissolved, as can be seen on the mineral image in Figure 10d. From this it was clear that RMA attacks the matrix too heavily, and will lead to matrix collapse. Treatment with HMA (half-strength mud acid) resulted in only partial dissolution of the calcite cement. The mineral image after this treatment can be observed in Figure 10f. In this case the permeability was greatly improved without reducing the strength of the matrix so much that collapse could occur.

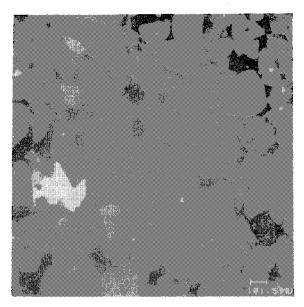


FIGURE 9a BSE image of a shaly sandstone with some dolomitic and pyritic cement $% \left(1\right) =\left(1\right) +\left(1\right) +\left($

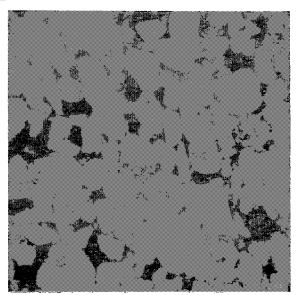


FIGURE 9b Mineral image derived from Figure 9a. Note the ankerite rims in red around the dolomite cementation in green.

(See Colour Plate IX at the back of this publication.)

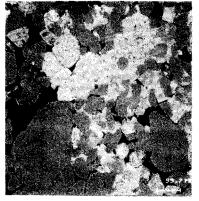


FIGURE 10a BSE image of a shaly sandstone with calcite cementation

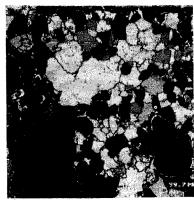


FIGURE 10b Mineral image of Figure 10a (See Colour Plate X at the back of this publication.)

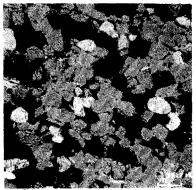
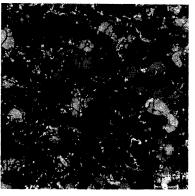


FIGURE 10c BSE image of the same sandstone FIGURE 10d Mineral image of Figure 10c. as shown in Figure 10a after treatment with RMA (regular mud acid)



Note the complete absence of the calcite cementation, which has been dissolved by the aggressive RMA. Also note the large amount of fines (small white particles) precipitated in the acidisation process. (See Colour Plate XI at the back of this publication.)

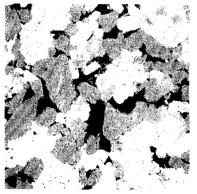
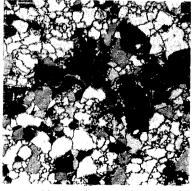


FIGURE 10e BSE image of the same sandstone FIGURE 10f Mineral image of Figure 10e. as shown in Figure 10a after treatment Note that the matrix structure is still with HMA (half-strength mud acid)



Note that the matrix structure is still intact while the amount of open porosity has substantially increased compared with Figures 10a and 10b.

(See Colour Plate XII at the back of this publication.)

CONCLUSIONS & RECOMMENDATIONS

An automatic rock characterization procedure has been developed. Reproducible, consistent and objective mineralogical analysis can now be carried out on many rock types. In addition, automatic pore structure analysis can be performed. This information will be useful in predicting rock petrophysical properties. The techniques developed add new scope to petrographic analyses, enabling the quantification of a number of parameters (bulk mineralogy, grain texture and pore structure) using a single approach. Applying these new procedures should reduce the time spent in performing tedious and labour-intensive manual measurements.

The mineral identication procedure has been improved in accuracy. The proportion of unclassified objects has been reduced from typically 8% to less than 1%. Accurate analysis of 'difficult' objects such as lithics and clay rims is now possible. The sample preparation is greatly improved and fully automated, which ensures a very reproducible and rapid result. At the cost of longer analysis time the mineralogical accuracy is increased.

Future work will comprise the extension of the number of minerals in the classification procedure by incorporating more elements and involving texture analysis and geometrical data. In addition, new X-ray analysis algorithms will be developed to decrease the required analysis time. Finally, the relationship between 2-D geometry and 3-D reservoir parameters will be assessed.

ACKNOWLEDGEMENTS

We wish to thank Len Dijkshoorn for the effort she put into the sample preparation procedure, without which it would not have been possible to maintain the high quality and accuracy of the analysis. We also wish to thank Gerrit Nitters for his help and the use of the data from the acidisation experiments. Finally we wish to thank Hajo van Hasselt for reviewing this paper and for his encouraging comments.

REFERENCES

Textbook

SERRA, J., 1982,

Image analysis and mathematical morphology: London, Academic Press, 610 pp.

Journal article

HALL, M.G. and LLOYD, G.E., 1981,

The SEM examination of geological samples with a semiconductor backscattered electron detector: Am. Mineral., v. 66, pp. 362-368.

Journal article

DILKS, A. and GRAHAM, S.C, 1985,

Quantitative mineralogical characterization of sandstones by backscattered electron image analysis: J. Sed. Petrology, v. 55, pp. 347-355.

Special publication

CLELLAND, W.D., KANTOROWICZ, J.D. and FENS, T.W, 1990,

Quantitative analysis of pore structure and its effect on reservoir behaviour: Upper Jurassic Ribble Sands, Fulmar Field, UK North Sea: In 'Advances in Reservoir Geology' (Eds. M. Ashton and J.D. Marshall), Geological Society of London.

Textbook

WEIBEL, E.R, 1980,

Stereological methods, Vol. 2. Theoretical foundations: London, Academic Press.

SPE proceedings

FENS, T.W & CLELLAND, W.D, 1990,

Automated rock characterisation using scanning electron microscopy/image analysis techniques: Europec 1990, SPE 20920, p. 369.

SPE proceedings

NITTERS, G. & HAGELAARS, A.M.P.M, 1990,

Careful planning and sophisticated laboratory support: the key to improved acidisation results: Europec 1990, SPE 20967, p. 289.